



Article

Thermodynamic and kinetic study of the adsorption of organic pollutants using environmentally friendly materials

¹Fadya Raheem Salih and ²Suhad S. Mohammed

1,2 Department of Chemistry, College of Education for Pure Sciences,
Ibn Al – Haitham, University of Baghdad, Baghdad, Iraq.

suhad.sh.m@ihcoedu.uobaghdad.edu.iq

fadia.saleh2205m@ihcoedu.uobaghdad.edu.iq

Abstract

An AFM and BET were used to diagnose Flint surface, and the results were displayed. where it was determined that the specific surface area of Flint is $6.2697 \text{ m}^2 \text{ g}^{-1}$. The biggest peak that may be obtained by a certain amount of Flint surface, with granules and an average diameter of 63.84 nm, is 31.0535 nm in height. The aqueous solution of Erythrosine was removed using the adsorption capabilities of Flint. The range of maximal dye adsorption was found to be 10.19-43.77%. At temperatures of (298,308,318,328)K, the Freundlich model was utilized since Temkin model could only be partially applied, Langmuir model was not appropriate, and the Freundlich model was the only one that worked. Reason being, out of the three models, it is the one that will be most useful in the real world. Physical adsorption is another option. Based on the results, the pseudo-second-order model, One of the three adsorption process kinetic models that were taken into consideration, was significantly applicable. Through the application of thermodynamic functions based on the enthalpy value, it was determined that the process was exothermic, with a negative value of -19.9471 kJ/mol. Similarly, the value of entropy was negative, which was -2.7962 J/mole.K. The process was shown to be exothermic adsorption, spontaneous, and occurring without randomization when Gibbs free energy was calculated.

Keywords: Removal; Pollution; Flint; Erythrosine; BET Surface Area.

1.Introduction

The term "pollutant" refers to any material—liquid, solid, or gaseous—that is introduced to the environment. Due to its pervasiveness in society, pollution ranks high among environmental and human concerns [1]. Disposal of many types of trash, including organic, petrochemical, petroleum, and industrial materials, is a common cause of this pollution [2].

Potential threats to human health include drinking water contaminated with organic dyes. Many worry that industrial dyes pose a threat to water quality. Contamination of the environment is still an issue, and it becomes much worse when the toxins are resistant and persistent. The xanthene family of synthetic colours is a subset of this category [3].

Clay is a major contributor to soil contamination because of the large amounts of toxins it can absorb. In organic pollution, clay particles often contain cations of innocuous elements like sodium and calcium, which can easily swap with toxic heavy metals like lead, cadmium, and mercury. Clay may be able to bind a significant number of organic pollutants due to its large surface area and capacity for a wide range of molecular interactions outside of ion exchange [4].

Flint is a soft, white mineral that has numerous uses. Porcelain makes extensive use of flint, which is abundant in Nigeria. Extensive study has demonstrated its efficacy in eliminating harmful metals from wastewater. It was found to be effective in removing nitrate, methylene blue, hexavalent chromium, and Congo Red from water-based solutions [5].

Synthetic dye from the xanthene family, is used as a food colorant [6]. The food sector, which includes the manufacturing of chocolate, biscuits, meat, candies, and chewing gum, as well as the pharmaceutical and cosmetics industries, make extensive use of Erythrosine (E127) as a colorant. [7]. With a solubility of 70g/L in water and excellent stability in both basic and neutral solutions, Erythrosine is a versatile drug. Fig.1 shows the chemical structure of synthetic E127 [8].

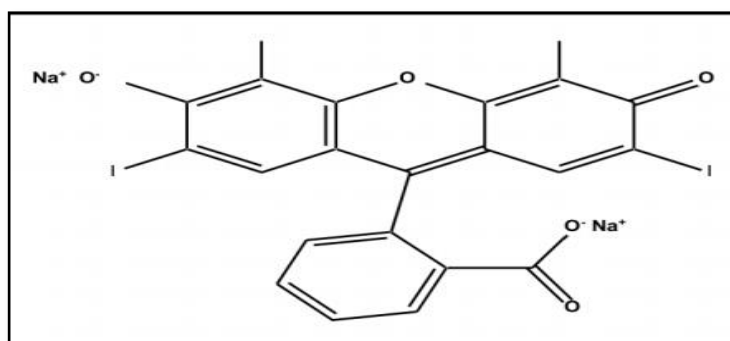


Figure 1. Chemical structure of Erythrosine [8].

2. Materials and method

2.1. Preparation of E127 stock solution

A standard solution was prepared by dissolving (1g) of E127 dye in de-ionized distilled water in a beaker. A 1000 ml volumetric flask was then used to dilute this solution. A solution of E127 was prepared with a concentration range of (5.0 - 50.0)ppm.

2.2. Preparation of Flint

An enough quantity was measured and transferred to a glass beaker to wash Flint clay. To further eliminate any surface impurities, the clay was rinsed ten to twelve times using de-ionized distilled water. Six hours were spent in a lab oven at 100 °C to dry the surface. Grind the dry surface with an electric grinder. With a granular size of (75µm), the Flint was passed through a molecular filter. Thereafter, it was preserved for the examination by placing it in a plastic container.

2.3. Diagnostics of the flint surface using Atomic Force Microscopy

Atomic force microscope (AFM) It is a high-resolution microscope that can produce two- and three-dimensional images of surfaces and analyze samples at a thousand times higher resolution than optical microscopes, which can only diagnose objects that are a few nanometers in size [9].

Fig2 shows the results of using AFM instrument to take two- and three-dimensional pictures of the surface topography of Flint. Investigating a sample that had been crushed using a sieve with a granular size of (75µm) or less yielded the following results:

As shown in Fig. 2, the highest height that a specific amount of Flint surface can reach is (31.0535)nm.

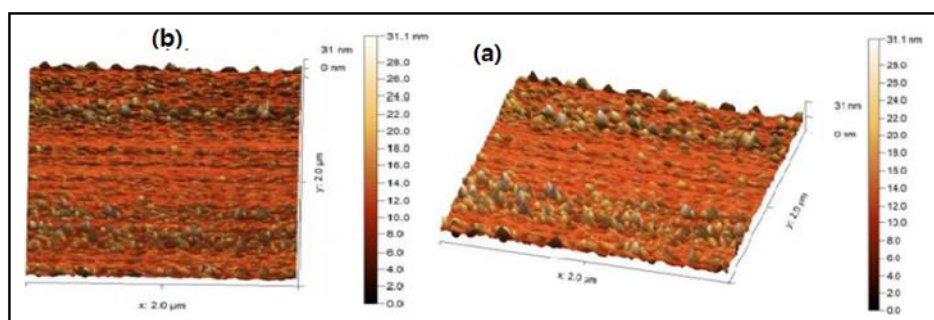


Figure 2. (a) 3D and (b) 2D image of Flint under AFM

According to the results of the particle analysis, the granules' distribution varied, and their diameters ranged from 57.35 nm to 76.32 nm, with an average of 63.84 nm. These findings are presented in Fig.3 and Scheme 1. In accordance with the chart's subsequent analysis. Many of the granules measured less than 70 nm in diameter, while bigger granules were sometimes present.

Many of the granules measured less than 70 nm in diameter, while bigger granules were sometimes present.

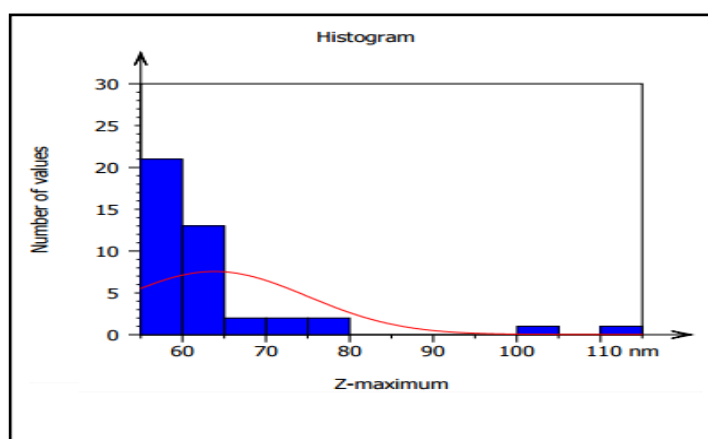
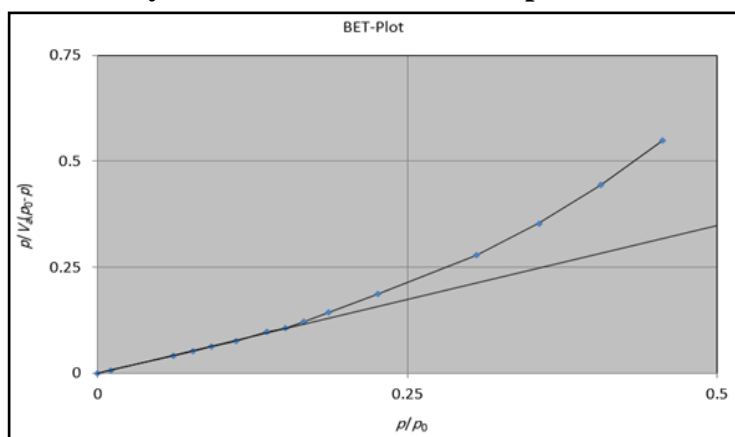


Figure 3. Analysis of data of Flint surface particles under AFM



Scheme1. The distribution of granules on Flint based on granule diameter.

2.4.BET Surface Area of Flint

The specific surface area (S_{BET}) for flint is determined by the N_2 adsorption and desorption isotherm at (77.00) K. The pore structure and BET adsorption desorption curve are shown in Fig.4. Based on the IUPAC classification system, it is shown that the adsorption-desorption isotherm curve belongs to Type IV, and Flint has a mesoporous pore shape. With a specific surface area of ($6.2697 \text{ m}^2 \text{ g}^{-1}$)

¹), an average pore width of (7.7947 nm), and a total pore volume of (0.0122 cm³ g⁻¹). [10]

Individual results		
Parameters	Projected area	Z-maximum
Unit	μm ²	nm
Particle #1	0.01566	76.32
Particle #2	0.002343	70.50
Particle #3	0.001481	72.69
Particle #4	0.002309	75.46
Particle #5	0.000248	60.39
Particle #6	6.151e-05	57.35
Particle #7	0.000125	57.82
Particle #8	6.536e-05	57.71
Mean	0.04509	63.84

Statistical summary					
Parameters	Unit	Mean	Std dev	Min	Max
Projected area	μm ²	0.04509	0.2065	6.151e-05	1.196
Z-maximum	nm	63.84	11.11	57.35	112.8

Figure 4. BET plot of Flint adsorption

2.5. Determination of the maximum wavelength (λ_{max}) for E127

The λ_{max} was found by using a standard solution of E127. A visible and ultraviolet spectrophotometer was used to measure it within the range of (190-800 nm). The greatest wavelength at which E127 absorbs light is (526 nm) nanometers. We utilized a quartz cell that was 1 cm thick for the measurement, Fig.5 shows E127 dye's absorption spectrum.

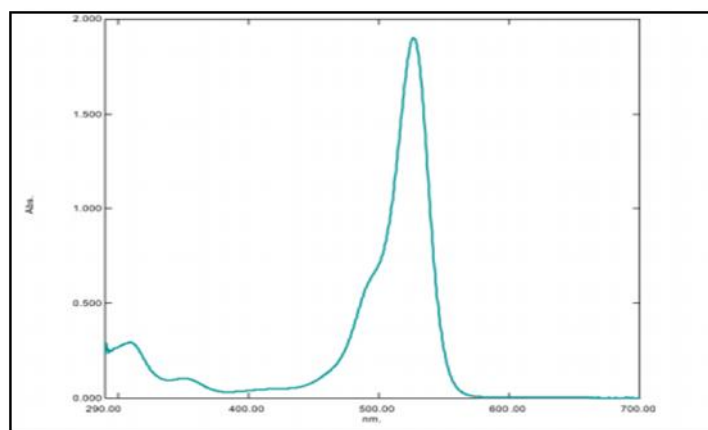


Figure 5. UV-visible absorption spectrum of E127

3.Results and Discussion

3.1. Impact of the adsorbent weight (Flint) on the capacity for adsorption

To find out how much weight the Flint should have to remove E127 dye via adsorption on its surface, we investigated a range of Flint weights from 0.05 to 0.7g at 298K with a primary dye concentration of 50mg/L. Fig.6 shows that the adsorbent surfaces were more successful in removing the dye from its water-based solution when the number of active sites generated Adsorption for E127 was raised. A steady increase in percentage of removal (%R) was seen as Flint weight increased by (0.05 to 0.9)g, or (10.19 to 43.77)%. All of the adsorption sites at Flint surface were saturated, which led to the percentage of elimination to remain constant at the optimal weight of (0.6)g. of Flint, which was (43.77)% [11].

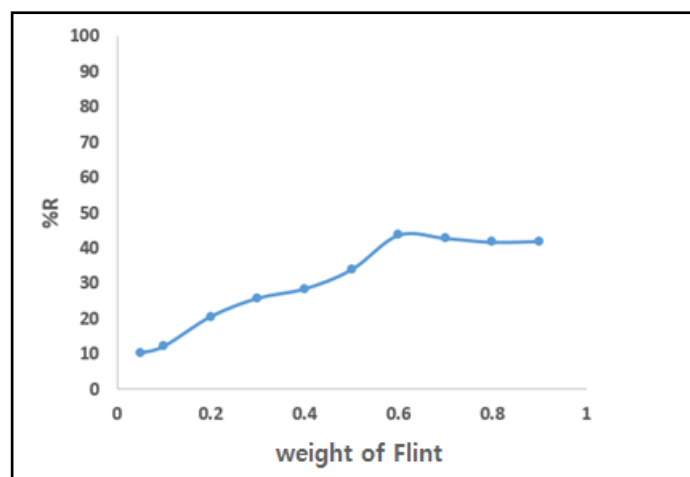


Figure 6. Flint's weight and its impact on the adsorption of E127

3.2. Determine the equilibrium time.

At initial dye concentrations of (50mg/L) and at different temperatures (298,308,318,328)K, The impacts of Flint's equilibrium time with the dye E127 aqueous solution for granule size ($\leq 75\mu\text{m}$) and Flint's ideal weight (0.6g) were investigated. Fig.7 shows the linear relationship between the passage of time and the adsorption process on Flint. According to the results, E127 dye adsorption process on Flint has an equilibrium duration of (40 min).

Figure 7. Effect of equilibrium time on the amount of E127 that was adsorbed on Flint

3.3. Adsorption Kinetics Models studies

Applying pseudo-first-order (PFO), pseudo-second-order (PSO), and Elovich kinetic models, the adsorptive behavior of E127 on Flint was examined. Here is the linear form of PFO that has been stated. [12]

$$\ln(q_e - qt) = \ln q_e - K_1 t \quad \text{_____} 1$$

qt in unite (mg/g) is capacity for adsorption at time, qe in unite (mg/g) is capacity for adsorption at equilibrium, and K1 is the rate constant for adsorption in unite (min⁻¹). To determine K1, we look at the linear plot of ln (qe-qt) against time (t), as shown in Fig.8a.

To find Pseudo first order constants, follows formula (2). [13]

$$\frac{t}{qt} = \frac{1}{K_2 q_e^2} + \frac{1}{q_e} t \quad \text{_____} 2$$

K₂ in unite (g mg⁻¹. min⁻¹) is (PSO) process's adsorption rate constant. The plot of t/qt vs. time (t) is linear, and K₂ is calculated from the intercept of this curve Fig.8b.

The (Elovich) constants are determined using the constants α and β as shown in formula (3). [14]

$$qt = \frac{1}{\beta} \ln(\beta\alpha) + \frac{1}{\beta} \ln t \quad \text{_____} 3$$

The desorption process constant is denoted by α and is measured in units of (mg.g⁻¹.tim⁻¹), while the initial adsorption rate constant is denoted by β and is measured in units of g.mg⁻¹. In addition, the values of are computed using the slope and intercept shown in Fig.8c. [15]

The strong (R²) values and converging of the theoretical and actual (qe) values make PSO and Elovich models usable; this is demonstrated by the results in Table1 and an examination of the R² values for the three Kinetic models. Real (qe) values didn't match theoretical values, and there were not enough (R²) values to use PFO Kinetic models. [16,17]

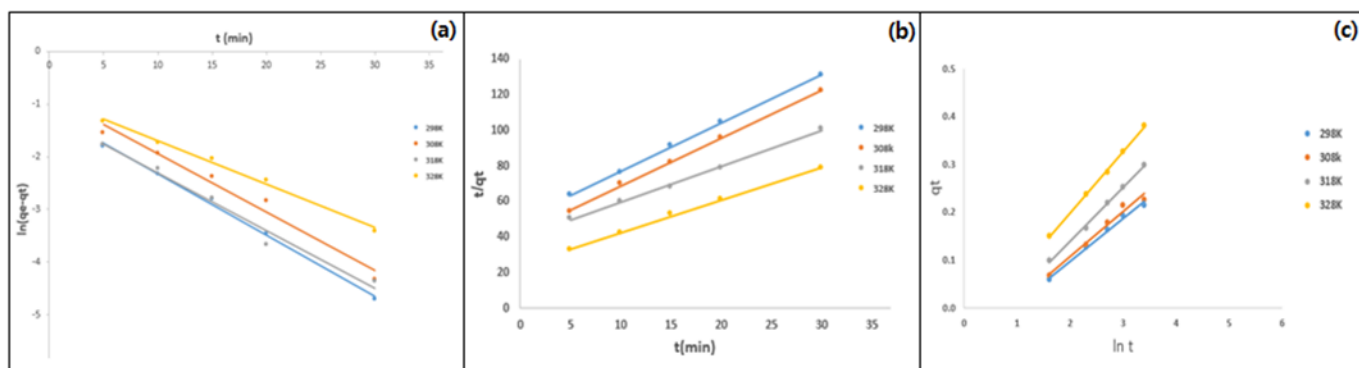


Figure 8. (a) PFO, (b)PSO, (c)Elovich kinetic models for the adsorption of E127 on Flint at different temperatures.

Table (1) Adsorbent Flint surface's kinetic constant values at various temperatures

T(K)	Pseudo first order			Pseudo second order			Elovich		
	K1 (min ⁻¹)	qe (mg/g)	R ²	K2 (g.mg ⁻¹ .min ⁻¹)	qe (mg/g)	R ²	β (g.mg ⁻¹)	α (mg.g ⁻¹ .min ⁻¹)	R ²
298	0.1163	0.313	0.997	0.1496	0.3667	0.9997	11.2107	0.0363	0.9913
308	0.1091	0.2955	0.9785	0.1716	0.3726	0.9989	10.6496	0.0398	0.9786
318	0.1105	0.4318	0.976	0.1021	0.4981	0.9977	8.8967	0.0527	0.9978
328	0.0823	0.4162	0.9923	0.1376	0.5469	0.9987	7.9064	0.0821	0.9987

3.4. Adsorption isotherms

We used a range of temperatures (298, 308, 318, and 328) K, various concentrations of E127 (5-60 mg/L), the optimal adsorbent surface weight of Flint (0.6 g), particle size ($\leq 75\mu\text{m}$), and an equilibrium time (40 min) to analyze the adsorption isotherms. Adsorption isotherms of E127 dye on Flint at various temperatures are shown in Fig.9 as a function of both $q_t(\text{mg/g})$ and $(C_e (\text{mg/L}))$.

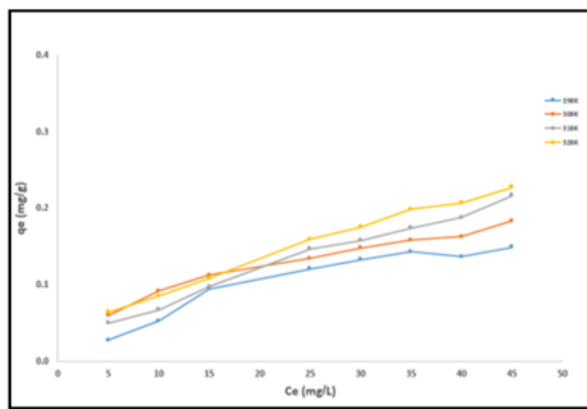


Figure 9. Isotherm for adsorption of E127 on Flint

In accordance with Freundlich's adsorption principles, the dye's adsorption curve on Flint type (L3) is depicted in Fig.9. In accordance with Giles' classification, this demonstrates that various forces are applied during the adsorption process on the adsorbent surface. The more area the adsorbent surface covers, the more material is adsorbed on the surface [18]. Because adsorption takes place horizontally on the adsorbent surface, the adsorbent will occupy a bigger part of the surface. Thus, occupied areas on the surface with limited adsorption potential and a small amount of adsorption will occur. [19]

3.5. Adsorption Isotherm Models

After analyzing the acquired data using three adsorption process isotherm models, The findings for the Temkin, Freundlich, and Langmuir model constants as well as correlation coefficients are shown in Table 2. Fig10 shows the adsorption isotherm models. Through the application of equation (4), Freundlich model constants K_f in unite (mg/g) and (n) were determined. [20]

$$\log(qe) = \log(Kf) + \frac{1}{n} \log Ce \quad \text{_____} 4$$

By applying formula (5), we were able to determine K_L in unit (L/mg) which represents Langmuir constants and q_{max} in unite (mg/g). [21]

$$\frac{Ce}{qe} = \frac{Ce}{qe \max} + \frac{1}{qe \max Kl} \quad \text{_____} 5$$

Applying formula (6), BT (J/mol) and Temkin constants in unit (L/mg) were taken into consideration. [22]

$$qe = BT * \ln KT + BT * \ln Ce \quad \text{_____} 6$$

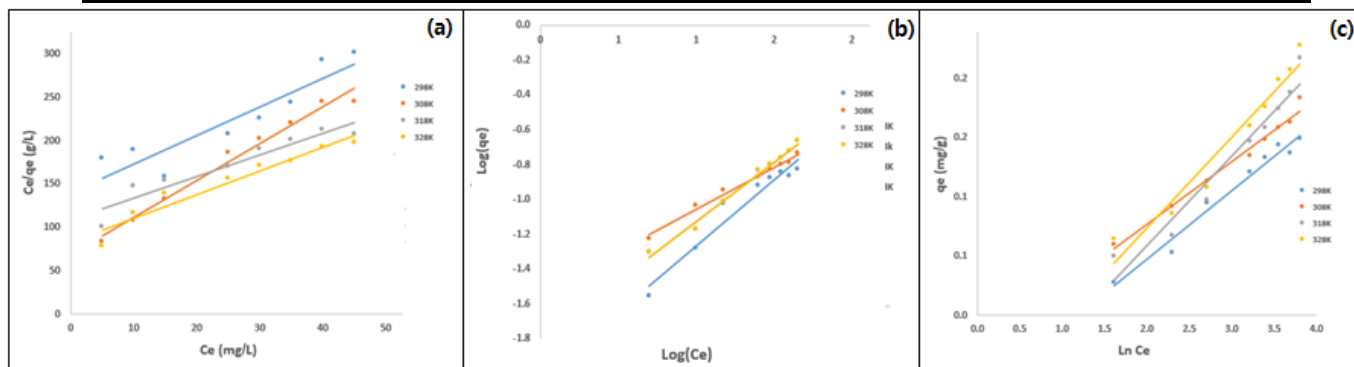


Figure 10. (a)Langmuir, (b)Freundlich, (c)Temkin isotherms for adsorption of E127 on Flint at different temperatures.

T(K)	Langmuir			Freundlich			Temkin		
	KL (L/mg)	qemax (mg/g)	R ²	Kf (mg/g)	n	R ²	KT (L/mg)	BT (J/mol)	R ²
298	0.0234	0.3035	0.8454	0.0093	1.3137	0.9482	0.5763	7.5354	0.976
308	0.0618	0.2346	0.9821	0.0291	2.0859	0.9883	0.3564	7.3207	0.9822
318	0.0227	0.4021	0.9037	0.0155	1.4641	0.9898	0.3068	5.9072	0.9447
328	0.0323	0.3684	0.9347	0.0228	1.6697	0.9901	0.2951	4.0026	0.9482

Table (2) The adsorbent surface Flint's isotherm constant values at various temperatures.

The adsorption process in this experiment may be well described by Freundlich's isotherm equation, as shown in Table 2, which also demonstrates that the values of (n) must be between 1 and 10. This demonstrates that physical forces control the adsorption process. Freundlich constant (Kf) for the adsorbent surface Flint decreases with increasing temperature, lending credence to the idea that the adsorption process is exothermic. There were several different adsorption energy locations on the heterogeneous surfaces where the adsorption process occurred [23]. Langmuir model does not fit, as shown in Table 2, due to the relatively low linear correlation coefficient at the same test temperatures [24]. Similarly, Temkin's model has limited applicability because the surface correlation coefficient is always less than 0.9. [25]

3.6. Thermodynamic study for adsorption of E127 on Flint

By calculating thermodynamic constants like Gibbs free energy, Entropy and Enthalpy (ΔG° , ΔS° , ΔH°), the impact of temperature on the adsorption process's behavior could be shown [26]. A look at Table 4. reveals the thermodynamic function values. E127 adsorption process's equilibrium constant on Flint was estimated by using Equation (7) to calculate the values of the thermodynamic functions at each temperature, which were necessary for the adsorption of dye on the adsorbent surface [27].

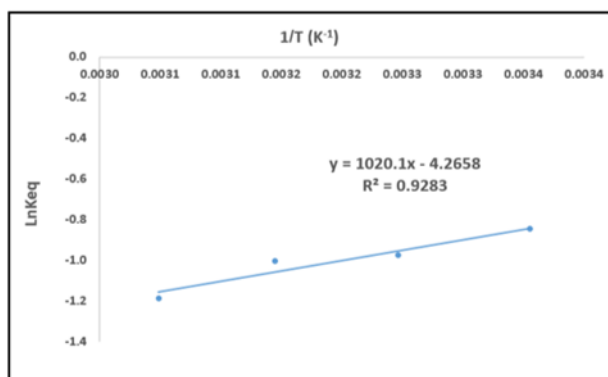


Figure 11. Vant Hof's equation for adsorption E127 dye on Flint

$$K_{eq} = \frac{q_e * W(g)}{C_e * V(l)} \text{ ----- } 7$$

Plotting Fig. 10 between lnKeq and 1/T from Table 3 will yield the equations for ΔH° and ΔS°. The slope is denoted by (- ΔH°/R) and the intercept by (ΔS°/R) [28].

$$\ln K_{eq} = \frac{-\Delta H^\circ}{RT} + \frac{\Delta S^\circ}{R} \text{ ----- } 8$$

Table (3) Thermodynamic values of E127 dye on the Flint at different temperatures.

Adsorbent	T (K)	ΔG° KJ/mole	ΔH° KJ/mole	ΔS° J/mole.k
Flint	298 K	-6.953	-19.9471	-2.7962
	308 K	-4.3169		
	318 K	-5.5058		
	328 K	-3.9068		

To calculate the change in Gibbs free energy, utilizes Equation (9) [29].

$$\Delta G^\circ = -RT \ln K_{eq} \text{ ----- } 9$$

Table (4) values of the adsorption E127 dye thermodynamic equilibrium constants at various temperatures and on Flint.

Adsorbent	T (K)	1/T (K ⁻¹)	K _{eq}	Ln K _{eq}
Flint	298 K	0.0034	0.2792	-1.2758
	308 K	0.0032	0.3874	-0.9483
	318 K	0.0031	0.3664	-1.004
	328 K	0.003	0.4257	-0.854

The enthalpy values were lower than 40 KJ/mol, confirming physical adsorption, and the fact that the adsorption process was exothermic shows that it occurred on

Flint [30]. The regularity, rather than randomness, of the surface dye adsorption process is demonstrated by the negative entropy values. It is not a spontaneous adsorption process for E127 dye on Flint because the Gibbs free energy values are positive [31].

Conclusions

The experiment showed that Flint absorbed Erythrosine dye with a removal rate of 43.77%. According to the results of the used kinetic constants, (PSO) model has the best match. matching Freundlich isotherm as an additional condition. The lack of spontaneity in the adsorption process is shown by the negative values of ΔG° , which, along with the negative values of ΔS° and ΔH° , suggests that the adsorption process is becoming more regular, is exothermic, and physical.

References

- [1] Nassar, N.N., Marei, N.N., Vitale, G. and Arar, L.A., [2015]: Adsorptive removal of dyes from synthetic and real textile wastewater using magnetic iron oxide nanoparticles: thermodynamic and mechanistic insights. *The Canadian Journal of Chemical Engineering*. 93(11), pp.1965-1974.
- [2] Abbas, A.M., Mohammed, Y.I. and Himdan, T.A., [2017]: Adsorption kinetic and thermodynamic study of congo red dye on synthetic zeolite and modified synthetic zeolite. *Ibn AL-Haitham Journal For Pure and Applied Science*.28(1), pp.54-72.
- [3] Mane, Sachin, Ponrathnam, Surendra, Chavan, N. [2015]: Selective solidphase extraction of metal for water decontamination. *Journal of Applied Polymer Science*. 133(10):42849.
- [4] Al-Taweel, S. S., Isa, S. A., & Al-Ani, R. R. [2018]: Three Locally Clays as A Surfaces for Adsorption of Cephalexin Monohydrate From Aqueous Solution: Thermodynamic and Desorption Equilibrium. *Ibn AL-Haitham Journal For Pure and Applied Sciences*. 195–205.
- [5] Ekekwe, E. D., Nnabuike, C. C., & Chibuzo, C. K. [2018]: Adsorption of zinc on Cassava peels activated carbon and kaolin clay: kinetics, thermodynamics, and optimization studies. *Adsorption*.
- [6] R. Bernstein, H. Haugen and H. Frey, *Scandinavian journal of clinical and laboratory investigation* 1975, 35, 49–52.
- [7] S. Bonan, G. Fedrizzi, S. Menotta and C. Elisabetta, [2013]: *Dyes and Pigments* 99, 36–40.
- [8] Al-Degs, Y. S., Abu-El-Halawa, R., & Abu-Alrub, S. S. [2012]: Analyzing adsorption data of Erythrosine dye using principal component analysis. *Chemical engineering journal*, 191, 185-194.
- [9] Binnig, G., Quate, C.F. and Gerber, C., [1986]: *Atomic force microscope*. *Physical review letters*, 56(9), p.930.

- [10] K. S. Sing, "Reporting Physisorption Data for Gas/Solid Systems With Special Reference to the Determination of Surface Area and Porosity (Recommendations 1984)," *Pure and Applied Chemistry* 57, no. 4 (1985): 603–619, <https://doi.org/10.1351/pac198557040603>
- [11] Fathi, M. R. : Asfaram, A., , Farhangi, A. [2015]: Removal of Direct Red 23 from aqueous solution using corn stalks: isotherms, kinetics, and thermodynamic studies. *Spectrochimica Acta Part A: Molecular and Biomolecular Spectroscopy*. 135, 364-372.
- [12] SA Suhad S. Mohammed, Lekaa K. Abdul Karem [2020]: Spectroscopic, Thermodynamic and Kinetic Studies of Ligand Complexes Derived From 2-Amino Thiophenol. *Biochemical and Cellular Archives*. 20(2), 6329-6334.
- [13] Simonin, J. P. [2016]: On the comparison of pseudo-first order and pseudosecond order rate laws in the modeling of adsorption kinetics. *Chemical Engineering Journal*. 300, 254-263.
- [14] Dawodu, F. A. , Akpomie, K. G. [2014]: Kinetic, equilibrium, and thermodynamic studies on the adsorption of cadmium (II) ions using "Aloji Kaolinite" mineral. *Pac. J. Sci. Technol*. 15, 268-276.
- [15] Mohammed, S. S. , Al-Heetimi, D. T. [2019]: Adsorption of Methyl Violet Dye from Aqueous Solution by Iraqi Bentonite and Surfactant-Modified Iraqi Bentonite. *Ibn AL-Haitham Journal For Pure and Applied Science*. 32(3), 28-42.
- [16] Karmaker, S. , Sintaha, F. , Saha, T. K. [2019]: Kinetics, isotherm, and thermodynamic studies of the adsorption of reactive red 239 dye from aqueous solution by chitosan 8B. *Advances in Biological Chemistry*. 9(01), 1.
- [17] Idris, S., Iyaka, Y. A., Ndamitso, M. M., Mohammed, E. B., & Umar, M. T. [2011]: Evaluation of kinetic models of copper and lead uptake from dye wastewater by activated pride of barbados shell. *American Journal of Chemistry*, 1(2), 47-51.
- [18] Sanz-Santos, E. , Álvarez-Torrellas, S. , Larriba, M. , Calleja-Cascajero, D. , García, J. [2022]: Enhanced removal of neonicotinoid pesticides present in the Decision 2018/840/EU by new sewage sludge-based carbon materials. *Journal of Environmental Management*. 313, 115020.
- [19] Karam, F.F., Saeed, N.H., Al Yasarri, A., Ahmed, L. and Saleh, H., [2020]: Kinetic study for reduced the toxicity of textile dyes (reactive yellow 14 dye and reactive green dye) using UV-A Light/ZnO system. *Egyptian Journal of Chemistry*, 63(8), pp.2987-2998.
- [20] Al-Kazragi, M. A., Al-Heetimi, D. T., & Al-Khazrajy, O. S. [2019]. Xylenol orange removal from aqueous solution by natural bauxite (BXT) and BXTHTMA: kinetic, thermodynamic and isotherm modeling. *Desalination Water Treat*, 145, 369-377.

- [21] Abbas, A. M., Mohammed, Y. I., & Himdan, T. A. [2017]: Adsorption kinetic and thermodynamic study of congo red dye on synthetic zeolite and modified synthetic zeolite. *Ibn AL-Haitham Journal For Pure and Applied Science*, 28(1), 54-72.
- [22] Boparai, H. K. , Joseph, M. , O'Carroll, D. M. [2011]: Kinetics and thermodynamics of cadmium ion removal by adsorption onto nano zerovalent iron particles. *Journal of hazardous materials*186(1), 458-465.
- [23] Ali, I. H. . [2021]: Removal of Congo Red Dye From Aqueous Solution Using Eco-Friendly Adsorbent of Nanosilica. *Baghdad Science Journal*, 18(2), 0366.
- [24] Nkansah, M. A. , Donkoh, M., Akoto, O. , Ephraim, J. H. [2019]: Preliminary studies on the use of sawdust and peanut shell powder as adsorbents for phosphorus removal from water. *Emerging Science Journal*. 3(1), 33-40.
- [25] Wang, Y. , Chen, N., Wei, W., Cui, J. , Wei, Z. [2011]: Enhanced adsorption of fluoride from aqueous solution onto nanosized hydroxyapatite by lowmolecular-weight organic acids. *Desalination*. 276(1-3), 161-168.
- [26] Sahmoune, M. N. [2019]:Evaluation of thermodynamic parameters for adsorption of heavy metals by green adsorbents. *Environmental Chemistry Letters*. 17(2), 697-704.
- [27] Umpierres, C. S., Prola, L. D., Adebayo, M. A., Lima, E. C., Dos Reis, G. S.,Kunzler, D. D., Benvenuti, E. V. [2017]: Mesoporous Nb₂O₅/SiO₂ material obtained by sol–gel method and applied as adsorbent of crystal violet dye. *Environmental technology*. 38(5), 566-578.
- [28] .Mousa, S. A. [2020]: The A Comparative Study of the Adsorption of Crystal Violet Dye from Aqueous Solution on Rice Husk and Charcoal. *Baghdad Science Journal*, 17(1(Suppl.)), 0295.
- [29] Abbas, A. M., Mohammed, Y. I., Himdan, T. A. [2017]:Adsorption kinetic and thermodynamic study of congo red dye on synthetic zeolite and modified synthetic zeolite. *Ibn AL-Haitham Journal For Pure and Applied Science*.28(1), 54-72.
- [30] Mohammed, S. S., Aziz, N. M., & Abdul Kareem, L. K. [2021]: Preparation and Diagnostics of Schiff Base Complexes and Thermodynamic Study for Adsorption of Cobalt Complex on Iraqi Attapulgitic Clay Surface. *Egyptian Journal of Chemistry*, 64(12), 6913-6920.
- [31] Sah, M. K., Edbey, K., EL-Hashani, A., Almshety, S., Mauro, L., Alomar, T.S., ... & Bhattarai, A. [2022]: Exploring the biosorption of methylene blue dye onto agricultural products: A critical review. *Separations*, 9(9), 256.
- [32] Mahmood, R.A. and Mohammed, S.S., 2023. Study Of Effect Adsorption Of E127 Dye By Iraqi Clay From Aqueous Solution. *Journal of Kufa for Chemical Sciences*, 3(1), pp.126-138.